PHYSICAL REVIEW A VOLUME 42, NUMBER 11 1 DECEMBER 1990

# Frequency-dependent electric polarization due to optical rectification: Computer simulation and semiclassical theory

M. W. Evans
*Theory Center, Cornell University, Ithaca, New York 14853*

G. Wagnière
*Physical Chemistry Institute, University of Zurich, Winterthurerstrasse 190, Zurich CH 8057, Switzerland*

(Received 9 July 1990)

The symmetry principles governing the nonlinear interaction of intense laser radiation with molecular ensembles show that dynamical interaction phenomena exist in the ensemble even though the induced frequency-dependent polarization could be purely imaginary and unobservable in the static limit. An example is computer simulated in the *S* enantiomer of bromochlorofluoromethane, showing clear effects on the orientational and rotational velocity correlation functions and by Fourier transforming these functions, the dielectric and far-infrared spectra. Conditions are suggested for its experimental observation and orders of magnitude calculated for the appropriate mediating tensors.

## INTRODUCTION

The interaction of intense electromagnetic radiation with molecular ensembles may be described using time-dependent perturbation theory, a quantum-mechanical approach that has led recently to the discovery of several new birefringence effects, exemplified by the forward[1–3] and inverse[4] magnetochiral effects. A symmetry classification of these effects has recently been proposed[5–9] in terms of group-theoretical statistical mechanics (GTSM) and its three principles.[10–12] This classification indicates the presence of several other analogous phenomena,[13–16] prominent among which is optical rectification,[17] a phenomenon of nonlinear optics which is treated in this paper with molecular-dynamics computer simulation. This simulation method is based on the incorporation of appropriate extra torques in the forces loop of a standard molecular dynamics program. It has been shown, furthermore, that these torques may contain a real component[18] when the corresponding induced polarization is purely imaginary,[4] implying that there is a frequency-dependent, dynamical, effect of the intense laser field even when there is no real part to the complex polarization. An example of a hidden variable dynamical phenomenon in the rectification effect is investigated here with computer simulation in the *S* enantiomer of bromochlorofluoromethane, a chiral ensemble. It is found that the real component of the torque gives rise to clear spectral effects, which can be measured experimentally, for example, in the far-infrared and higher frequency regions of the electromagnetic spectrum.

## I. FREQUENCY-DEPENDENT POLARIZATION DUE TO OPTICAL RECTIFICATION

The quantum-mechanical expression for optical rectification has been given explicitly by Ward.[19] This expression for the purely real, static, electric polarization induced to second order by the radiation consists of double sums over all eigenstates of the unperturbed molecular system. The individual terms in these sums contain, in the numerators, products of matrix elements of the system-field interaction. The transition energies of the system, the frequency of the radiation field, and appropriate damping factors[19] appear in the denominators.

If one is primarily interested in the symmetry properties of the effect, it is therefore sufficient to consider the numerators, which are of general form:

$$\boldsymbol{\mu}(\boldsymbol{\mu}'\cdot\mathbf{E}_-)(\boldsymbol{\mu}''\cdot\mathbf{E}_+)\ , \tag{1}$$

where $\boldsymbol{\mu}$, $\boldsymbol{\mu}'$, and $\boldsymbol{\mu}''$ designate matrix elements of the electric dipole operator and $\mathbf{E}_-$ and $\mathbf{E}_+$ are electric field vectors complex conjugate to each other. Upon isotropic averaging, expression (1) splits up into a real factor pertaining to the molecular susceptibility multiplied by a field factor

$$(\boldsymbol{\mu}\cdot\boldsymbol{\mu}'\times\boldsymbol{\mu}'')(\mathbf{E}_-\times\mathbf{E}_+)\ . \tag{2}$$

This field factor $\mathbf{E}_-\times\mathbf{E}_+$ either vanishes if the radiation is linearly polarized, or is imaginary in the case of circular polarization. Even in an optically active fluid, the induced electric dc polarization is therefore not directly observable.

However, the polarization induced in the individual molecules couples to the electromagnetic field, resulting in a torque of generic form

$$\langle \mathcal{T}_k \rangle = \langle (\beta_{ijk} E_j E_k)(E_j) \rangle\ , \tag{3}$$

where $\beta_{ijk}$ has the units of the molecular hyperpolarizability tensor, with 27 scalar elements in general. This torque contains real contributions that do not average out in the ensemble.[18] Its dynamic influence may be interpreted on the basis of group-theoretical statistical mechanics.[10–12]

The tensor $E_jE_k$ (with nine scalar elements in general)

 

may be decomposed into a trace (rank-zero tensor) component $D^{(0)}$ under $R_3$, an axial vector (rank-one tensor) transforming as $D^{(1)}$, and a symmetric rank-two tensor, transforming as

$$\langle \mathcal{T} \rangle_0 = \langle (\beta \mathbf{E}_- \cdot \mathbf{E}_+) \times \mathbf{E}_\pm \rangle \ , \tag{4}$$

$$\langle \mathcal{T} \rangle_1 = \langle (\beta \mathbf{E}_- \times \mathbf{E}_+) \times \mathbf{E}_\pm \rangle \ , \tag{5}$$

$$\langle \mathcal{T} \rangle_2 = \langle (\beta \mathbf{E}_- \mathbf{E}_+) \times \mathbf{E}_\pm \rangle \ . \tag{6}$$

Assuming a plane wave as described by expression (8) below, we notice that if the radiation is linearly polarized and $\mathbf{E}_\pm$ is real, then $\langle \mathcal{T} \rangle_0$ will be real, $\langle \mathcal{T} \rangle_1$ will vanish, and $\langle \mathcal{T} \rangle_2$ may be made to vanish by an appropriate choice of the laboratory coordinate system. If the radiation is circularly polarized, then $\mathbf{E}_- = (\mathbf{E}_+)^*$ is complex. Both $\langle \mathcal{T} \rangle_0$ and $\langle \mathcal{T} \rangle_1$ will be complex and contain real contributions; $\langle \mathcal{T} \rangle_2$ will vanish for a circularly polarized wave as given by expression (4).

The torque $\langle \mathcal{T} \rangle$ in a circularly polarized laser thus has both real and imaginary parts. In consequence, the real part of a torque component such as $\langle (\beta \mathbf{E}_-^{(L)} \times \mathbf{E}_+^{(L)}) \times \mathbf{E}_\pm^{L,R} \rangle$ has a dynamical effect on the ensemble which can be observed numerically in the time correlation functions and experimentally in their Fourier transforms revealed as measurable spectra. It is a dynamical effect because the induced polarization vanishes at zero frequency.

## II. COMPUTER SIMULATION

Computer simulation of this dynamical effect proceeds as outlined in the Appendix of Ref. 17. In the simulation we have illustrated the effect by confining attention to the torque component:

$$\langle \mathcal{T} \rangle_1 = \langle (\beta \mathbf{E}_-^{(L)} \times \mathbf{E}_+^{(L)}) \times \mathbf{E}_+^{(L)} \rangle \ , \tag{7}$$

where $(R)$ and $(L)$ denote right or left circularly polarized, and the plus or minus igns denote complex conjugates of the field.[17] This gives the four possibilities:

$$\begin{aligned} &\mathbf{E}_-^{(L)} = E_0(\mathbf{i} + i\mathbf{j}) e^{-i\theta_L}, \quad \mathbf{E}_-^{(R)} = E_0(\mathbf{i} - i\mathbf{j}) e^{-i\theta_R} \ , \\ &\mathbf{E}_+^{(L)} = E_0(\mathbf{i} - i\mathbf{j}) e^{i\theta_L}, \quad \mathbf{E}_+^{(R)} = E_0(\mathbf{i} + i\mathbf{j}) e^{i\theta_R} \ , \end{aligned} \tag{8}$$

where

$$\theta_L = \omega t - \mathbf{K}_L \cdot \mathbf{r}, \quad \theta_R = \omega t - \mathbf{K}_R \cdot \mathbf{r} \tag{9}$$

are the phases in IUPAC convention.

The simulation proceeds by approximating the phases by

$$\theta \approx \theta_L = \theta_R = \omega t \tag{10}$$

and incorporating the real part of the torque into the forces loop of the program TETRA,[20] coded for 108 molecules of $(S)$ bromochlorofluoromethane, a chiral ensemble.[21] The torque (7) involes independent scalar elements of the molecular hyperpolarizability in the correct $C_1$ symmetry, which in the absence of known experimental or *ab initio* numerical data were coded in from data on methane. This procedure was adopted only *to illustrate the presence of the effect* in one of the simplest available chiral ensembles, and further work would involve the *ab initio* computation of all molecule fixed frame, scalar elements using a modification of a package such as HONDO.[22]

The molecules interacted with a site-site potential,[16,23]

$$\phi_{ij} = \sum_j \sum_i \left\{ 4\epsilon \left[ \left[ \frac{\sigma}{r_{ij}} \right]^{12} - \left[ \frac{\sigma}{r_{ij}} \right]^{6} \right] + \frac{q_i q_j}{r_{ij}} \right\} , \tag{11}$$

$$\sigma(\text{C-C}) = 3.4 \text{ Å}, \quad \frac{\epsilon}{k}(\text{C-C}) = 35.8 \text{ K},$$

$$\sigma(\text{H-H}) = 2.8 \text{ Å}, \quad \frac{\epsilon}{k}(\text{H-H}) = 10.0 \text{ K},$$

$$\sigma(\text{F-F}) = 2.7 \text{ Å}, \quad \frac{\epsilon}{k}(\text{F-F}) = 54.9 \text{ K},$$

$$\sigma(\text{F-F}) = 2.7 \text{ Å}, \quad \frac{\epsilon}{k}(\text{F-F}) = 54.9 \text{ K},$$

$$\sigma(\text{Br-Br}) = 3.9 \text{ Å}, \quad \frac{\epsilon}{k}(\text{Br-Br}) = 218.0 \text{ K},$$

$$\sigma(\text{Cl-Cl}) = 3.6 \text{ Å}, \quad \frac{\epsilon}{k}(\text{Cl-Cl}) = 158.0 \text{ K},$$

$$q(\text{C}) = 0.335|e|, \quad q(\text{H}) = 0.225|e| \ ,$$

$$q(\text{F}) = -0.22|e|, \quad q(\text{Cl}) = -0.18|e| \ ,$$

$$q(\text{Br}) = -0.16|e| \ ,$$

and their rotational and translational equations of motion were integrated with a time step of 50.0 fs on the CNSF IBM 3090-6S computer. The orientation and rotational velocity autocorrelation functions (ACF's) of the ensemble were evaluated in the field applied steady state using two field frequencies of 10.0 and 1.0 THz, respectively. These are roughly similar to the frequency of a $Q$-switched $CO_2$ laser. The correlation functions were evaluated in contiguous segments with running time averaging. The laser fields employed were powerful enough to show clearly the presence of changes in the time dependence of correlation functions (and thus in the frequency dependence of band shapes) and were energetically equivalent to about 25 kJ/mol at a temperature of 293 K at 1 bar.

## III. RESULTS: SPECTRAL EFFECTS DUE TO OPTICAL RECTIFICATION

Figure 1 illustrates the orientational ACF of the permanent molecular dipole moment for the $S$ enantiomer and recemic mixture. This is defined by

$$C_1(t) = \langle \mu_{0i}(t) \mu_{0j}(0) \rangle / \langle \mu_0^2 \rangle \ , \tag{11}$$

where $\langle \ \rangle$ denote ensemble averaging and where $\mu_0$ denotes the permanent molecular electric dipole moment. In this field-free equilibrium there are no orientational cross correlation functions (CCF's), which are off-diagonal elements of Eq. (11). Figure 2 is the same CF for an applied field of 1.0 THz, and Fig. 3 for 10.0 THz, each in the $S$ enantiomer. At the lower frequency, anisotropy in the orientational ACF components is clearly visible for a laser beam propagating in the $Z$ axis of $(X, Y, Z)$.

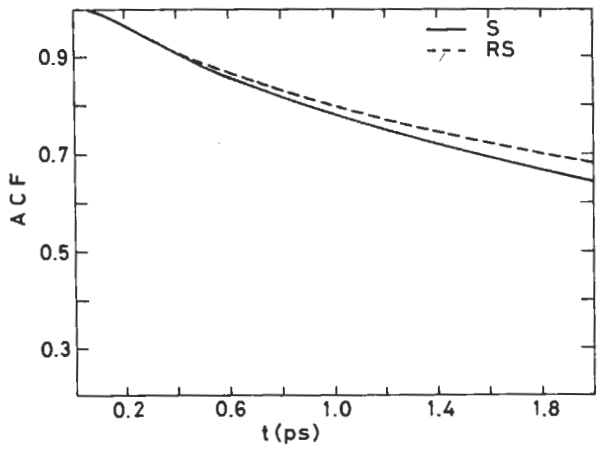


FIG. 1. Orientational ACF for *S*-bromochlorofluoromethane (*S*) and the racemic mixture (*RS*) at field-free equilibrium.

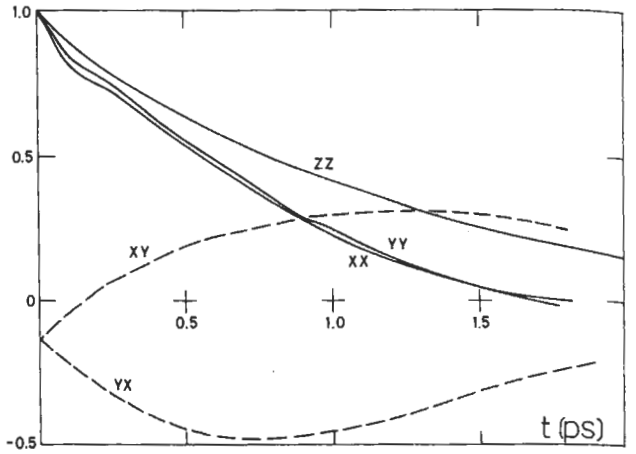


FIG. 3. As for Fig. 1 with the field frequency decreased to 0.01 THz. Note the development of anisotropy in the ACF's.

This is accompanied by the development of off-diagonal CCF elements of orientation as illustrated. At the higher frequency (Fig. 3), the anisotropy is lessened considerably, but the time dependencies of the ACF elements are clearly different from the average at field-free equilibrium (Fig. 1). Figure 3 also shows the presence of four off-diagonal CCF elements of orientation in the field applied steady state.

Figure 4 is the rotational velocity ACF at field-free equilibrium in the *S* enantiomer, defined by

$$C_2(t)=\langle \dot{\mu}_{0i}(t)\dot{\mu}_{0j}(0)\rangle / \langle \dot{\mu}_0^2\rangle \ . \tag{12}$$

Figure 5 is the equivalent in the steady state with an applied 1.0 THz field, and Fig. 6 for a 10.0-THz field. There is a clear effect at both frequencies, at 10.0 THz the ACF becomes highly oscillatory, and at the lower frequency Fig. 5 illustrates the development of interesting asymmetric CCF elements, reminiscent of those simulated by Evans and Heyes[24] in the context of Couette flow. The rotational velocity ACF is essentially part of the Fourier transform of the far-infrared frequency spectrum of the ensemble (power absorption coefficient and frequency-dependent refractive index), and in consequence, time-resolved techniques and powerful laser pulse trains can be used to evaluate experimentally the effect of electric (i.e., $\mathbf{E}_-\times\mathbf{E}_+$) rectification, a nonlinear "hidden variable" dynamical effect in the far-infrared and higher frequencies into the visible and beyond. Right and left circularly polarized pulse trains from a power laser are sent down the two arms of a Rayleigh interferometer, and the sensitivity of the instrument is used to measure the refractive and absorption index changes due to the various hidden variable effects exemplified in this paper. The sensitivity of this instrument can reach one part in one hundred million under practical conditions. The spectral resolution of the new "hidden variable" effect is achieved with a combination of Michelson and Rayleigh interferometers, the former being used to analyze the frequency dependence of the axial birefringence of the hidden variable effect, the latter as a sensitive measuring instrument of small differences in refractive index. The combined interferogram at the detector is made up of the

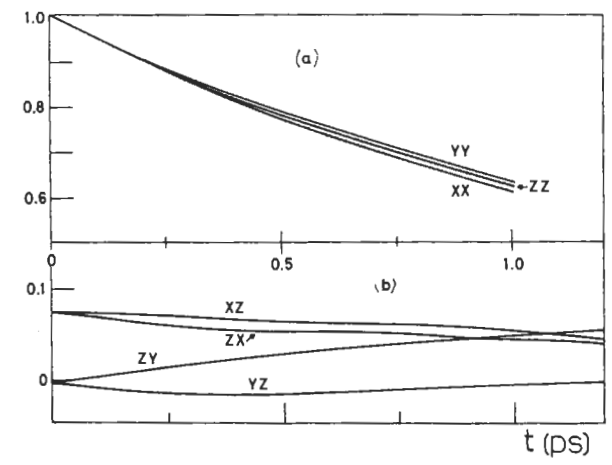


FIG. 2. As for Fig. 1 with the torque (3) applied at a field frequency of 10.0 THz. (a) Autocorrelation functions; (b) cross correlation functions.

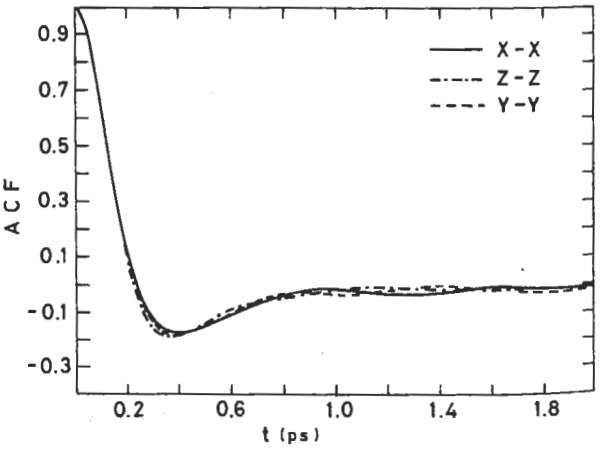


FIG. 4. As for Fig. 1, rotational velocity ACF, three diagonal components of the *S* enantiomer at field-free equilibrium.

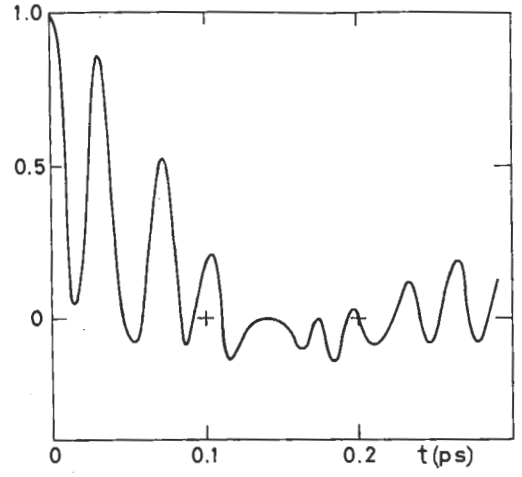


FIG. 5. As for Fig. 4 with torque (3) applied at 10.0 THz.

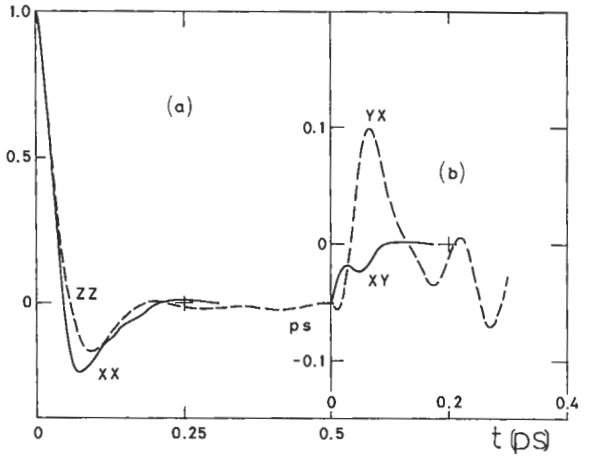


FIG. 6. As for Fig. 4, torque (3) applied at 0.01 THz. (a) Two of the diagonal (ACF) components; (b) two of the off-diagonal (CCF) components.

Michelson interferogram, as in a contemporary Bomem, Nicolet, or Bruker design, and the Rayleigh interferogram, a Fraunhoffer pattern from the input slits of the Rayleigh interferometer. The same setup can be used to detect magnetochiral birefringence, and, with a piezo-optic modulator, circular dichroism. This instrument is presently being developed.

## IV. MOLECULAR PROPERTY TENSORS AND ORDER OF MAGNITUDE ESTIMATES

In order to estimate the order of magnitude of the molecular property tensor mediating the effect of the conjugate product

$$\Pi=\mathbf{E}_{+}^{(L)}\times\mathbf{E}_{-}^{(L)}=-\mathbf{E}_{+}^{(R)}\times\mathbf{E}_{-}^{(R)}=2E_0^2 i\mathbf{k} \tag{13}$$

on the spectral features in Figs. 1 to 5, we use standard semiclassical theory[25] with an interaction Hamiltonian

$$\Delta H=-\frac{1}{2!}(\mathbf{E}_\alpha\times\mathbf{E}_\beta)\alpha_{\alpha\beta}\ . \tag{14}$$

The axial conjugate product vector $\Pi$ is negative to motion reversal $T$ and positive to parity inversion $P$, and is equivalent to a second rank antisymmetric polar tensor. A real, scalar, Hamiltonian is obtained from the tensor $(\Pi_{\alpha\beta})$ by contraction with another $T$ negative, $P$ positive, antisymmetric dynamic polarizability tensor[25]

$$\alpha_{\alpha\beta}\equiv\alpha'_{\alpha\beta}-i\alpha''_{\alpha\beta}\ . \tag{15}$$

The Hamiltonian (14) is therefore

$$\Delta H=-\Pi_z\alpha_z/2!=-E_0^2(\alpha''_{xy}-\alpha''_{yx})\ , \tag{16}$$

where $\alpha_z$ is the orbital or spin electronic polarizability, proportional to the sum of orbital $(\mathbf{L})$ and spin $(2\mathbf{S})$ electronic angular momenta:

$$\alpha=\gamma_\pi(\mathbf{L}+2\mathbf{S})\ . \tag{17}$$

From the time-dependent Schrödinger equation

$$\alpha''_{\alpha\beta}=-\alpha''_{\beta\alpha}$$
$$=-\frac{2}{\hbar}\sum_{\substack{j,n\\ j\neq n}}\frac{\omega}{\omega_{jn}^2-\omega^2}\,\mathrm{Im}(\langle n|\mu_\alpha|j\rangle\langle j|\mu_\beta|n\rangle) \tag{18}$$

for a transition from state $n$ to $j$ at the frequency

$$\omega_{jn}=\omega_j-\omega_n\ , \tag{19}$$

where $\mu_{\alpha,\beta}$ are electric dipole moments.

The product $\Pi$ is clearly independent of the phase of the electromagnetic field, but is generated by a frequency dependent electromagnetic field. The time dependent Schrödinger equation must be used, therefore, to find an expression for the $T$ and $P$ negative molecular property tensor $X_{ij}$ that mediates the induction of a dynamic molecular dipole moment $\mu_i$ by the conjugate product $\Pi_j$:

$$\mu_i=X_{ij}\Pi_j+\cdots\ . \tag{20}$$

Elementary time dependent perturbation theory expresses the tensor in the form

$$X_{\alpha\beta}=\frac{2}{\hbar}\sum_{\substack{j,n\\ j\neq n}}\frac{\langle n|\mu_\alpha|j\rangle\langle j|\alpha_\beta|n\rangle}{\omega_{jn}}\ , \tag{21}$$

where $\alpha_\beta$ is given in Eq. (18).

Note that this is $T$ and $P$ negative, and for an electronic vector polarizability $\alpha$ of the order $10^{-38}\ \mathrm{J^{-1}\,C^2\,m^2}$; a dipole moment of the order $10^{-30}\ \mathrm{C\,m}$; and for a transition frequency of the order $10^{15}\ \mathrm{rad\ s^{-1}}$; its order of magnitude is about $10^{-51}\ \mathrm{C^3\,m^3\,J^{-2}}$, about the same as that of the first electric hyperpolarizability. However, $X_{\alpha\beta}$ differs from the customary $\gamma_{ijk}$ because the latter is observable in achiral and chiral ensembles, and has a nonvanishing static component. The new dynamic property tensor $X_{\alpha\beta}$ appears only in chiral ensembles because of parity conservation. If observed in achiral ensembles there would be parity nonconservation, itself an important effect.

Finally we express the analogous[4] inverse Faraday

effect (experimentally observed magnetization due to $\Pi$) through the closely related molecular property tensor $Y_{ij}$:

$$m_i = Y_{ij}\Pi_j + \cdots , \tag{22}$$

where $m_i$ is the magnetic dipole moment due to $\Pi_j$. Perturbation theory gives the result

$$Y_{\alpha\beta} = \frac{2}{\hbar} \sum_{\substack{j,n \\ j\neq n}} \frac{\langle n|m_\alpha|j\rangle\langle j|\alpha_\beta|n\rangle}{\omega_{jn}} , \tag{23}$$

which is similar to Wagnière's equation (18) of Ref. 4 for the paramagnetic contribution to the inverse Faraday effect, in which equation the equivalent of spin polarizability is expressed through the cross product of electric dipole moments.

Equations (21) and (23) compare directly the new effect of this paper and the well-known inverse Faraday effect. The latter occurs in all ensembles, because the symmetry of $\Pi_j$ is the same as that of the $T$ negative, $P$ positive magnetic dipole moment $m_i$, so that $Y_{ij}$ is $P$ positive, $T$ positive. The inverse Faraday effect is much smaller than the new effect of Eq. (21), implying that the latter is easily observable by using, for example, dielectric spectroscopy, with pulses of circularly polarized neodymium-doped yttrium aluminum garnet (Nd:YAG) laser radiation to generate $\Pi_j$. The induced dynamic polarization is picked up as a dielectric loss in a capacitance-inductance circuit of the type used in nonlinear dielectric spectroscopy,[26] for example, with the strong electric field replaced by the pulsed and circularly polarized Nd:YAG pump laser.

## ACKNOWLEDGMENTS

This research was conducted using the resources of the Center for Theory and Simulations for Science and Engineering (Cornell Theory Center), which receives major funding from the National Science Foundation (U.S.) and I.B.M. Corporation, with additional support from New York State and Members of the Corporate Research Institute.

[1]G. Wagnière and A. Meier, Chem. Phys. Lett. **93**, 78 (1982).
[2]G. Wagnière and A. Meier, Experientia **39**, 1090 (1983).
[3]G. Wagnière and A. Meier, Z. Naturforsch. **39**, 254 (1984).
[4]G. Wagnière, Phys. Rev. A **40**, 2437 (1989).
[5]M. W. Evans, Phys. Lett. A **146**, 185 (1990).
[6]M. W. Evans, Phys. Rev. Lett. **64**, 2909 (1990).
[7]M. W. Evans, J. Modern Opt. **37**, 1655 (1990).
[8]M. W. Evans, Phys. Lett. A **146**, 485 (1990).
[9]M. W. Evans, Chem. Phys. **143**, 90 (1990).
[10]M. W. Evans, Phys. Lett. A **134**, 409 (1989).
[11]M. W. Evans, Phys. Rev. A **39**, 6041 (1989).
[12]M. W. Evans, Mol. Phys. **67**, 1195 (1989).
[13]M. W. Evans, J. Chem. Phys. **76**, 5473 (1982); **76**, 5480 (1982).
[14]M. W. Evans, P. Grigolini, G. Pastori, I. Prigogine, and S. A. Rice (eds.), *Advances in Chemical Physics* (Wiley Interscience, New York, 1985), Vol. 62, Chap. 5.
[15]M. W. Evans, Physica **131B&C**, 273 (1985).
[16]M. W. Evans, G. C. Lie, and E. Clementi, Z. Phys. D **7**, 397 (1988).
[17]M. Bass, P. A. Franken, J. F. Ward, and G. Weinreich, Phys. Rev. Lett. **9**, 446 (1962).
[18]M. W. Evans, Phys. Rev. A **41**, 4601 (1990).
[19]J. F. Ward, Rev. Mod. Phys. **37**, 1 (1965).
[20]M. W. Evans and M. Ferrario, Chem. Phys. **72**, 141 (1982); **72**, 147 (1982).
[21]M. W. Evans, I. Prigogine and S. A. Rice, *Advances in Chemical Physics* (Wiley Interscience, New York, 1985), Vol. 63.
[22]*Modern Techniques in Computational Chemistry*, edited by E. Clementi (Escom, Leiden, 1989).
[23]M. W. Evans, Phys. Rev. Lett. **50**, 37 (1983).
[24]M. W. Evans and D. M. Heyes, Mol. Phys. **65**, 1441 (1988).
[25]L. D. Barron, *Molecular Light Scattering and Optical Activity* (Cambridge University Press, Cambridge, 1982).
[26]M. Davies, *Dielectric and Related Molecular Processes* (Chemical Society, London, 1972–1977), Vols. 1–3.